UNIVERSITY OF CAPE TOWN

MASTER'S THESIS

QCD Boltzmann Equation: Beyond the soft-scattering approximation

Author:
Nicole MOODLEY

Supervisor:
Prof. Andre PESHIER

A thesis submitted in fulfillment of the requirements for the degree of Master of Science

in the

Department of Physics

October 16, 2022

Declaration of Authorship

I, Nicole Moodley, declare that this thesis titled, "QCD Boltzmann Equation: Beyond the soft-scattering approximation" and the work presented in it are my own. I confirm that:

- This work was done wholly or mainly while in candidature for a research degree at this University.
- Where any part of this thesis has previously been submitted for a degree or any other qualification at this University or any other institution, this has been clearly stated.
- Where I have consulted the published work of others, this is always clearly attributed.
- Where I have quoted from the work of others, the source is always given. With the exception of such quotations, this thesis is entirely my own work.
- I have acknowledged all main sources of help.
- Where the thesis is based on work done by myself jointly with others, I have made clear exactly what was done by others and what I have contributed myself.

Signed: Signed by candidate

Date:

University of Cape Town

Abstract

Faculty of Science
Department of Physics

Master of Science

QCD Boltzmann Equation: Beyond the soft-scattering approximation

by Nicole MOODLEY

In this thesis we use the case study of a spatially homogeneous many-gluon system, distributed isotropically in momentum space, to study the evolution of a hot (quark-) gluon plasma from an initial state towards equilibrium. To that end, we investigate the QCD Boltzmann equation making use of a calculation scheme that reproduces the known result for scalar interactions and generalizes to a QCD interaction, under an approximation of soft scattering.

Contents

Chapter 1

Introduction

1.1 Heavy-Ion Collisions and the QGP

Heavy-ion collision experiments, as performed at the Relativistic Heavy Ion Collider (RHIC) and the Large Hadron Collider (LHC), have been able to produce a previously only theorized state of matter known as the quark-gluon plasma (QGP) [1, 2]. These collisions generate energy density conditions so extreme that colour neutral hadrons dissociate into a highly dense mixture of their constituent quarks and gluons, whose interactions are governed by the theory of quantum chromodynamics (QCD). Studying QGP therefore gives us an opportunity to use both theoretical and experimental probes to better understand one of the fundamental forces of nature.

There is compelling experimental evidence that the QGP we are able to produce exhibits bulk properties, displaying behaviour associated with a "strongly coupled" near-perfect fluid. Consequently, naive applications of perturbative QCD are not well suited to describing many observables, as an assumption that the coupling constant be vanishingly small is questionable. Thus, is we wish to more broadly study QGP, we must go beyond standard perturbation theory.

One such method of studying QGP is through relativistic viscous hydrodynamics which, despite being able to successfully describe many bulk observables [3], is unable to ask (and therefore answer) questions about the nature of the interactions that drive the dynamcis of the QGP. In this thesis we shall be using its more fundamental alternative – relativistic kinetic theory.

1.2 Notation and conventions

We will use "natural units" with $c = \hbar = k_B = 1$, and Planck's constant $h = 2\pi$.

Euclidean vectors will be written in boldface, the components of which will be labeled by Latin indices as

$$\boldsymbol{x} = (x_1, x_2, x_3) = x_i \ .$$

Minkowski 4-vectors will be capitalized, with components labeled by Greek indices as

$$X_\alpha = (x_0, \boldsymbol{x}) \ .$$

Our choice of the Minkowski metric is

$$g_{\mu\nu} := \begin{pmatrix} 1 & 0 & 0 & 0 \\ 0 & -1 & 0 & 0 \\ 0 & 0 & -1 & 0 \\ 0 & 0 & 0 & -1 \end{pmatrix}$$

We write the 4-momentum with components $K = (E, \boldsymbol{k})$, where $E = K_0 = \sqrt{\boldsymbol{k}^2 + m^2}$ and the normalization is set to $m^2 = K_\mu K^\mu$. Fixed values will be denoted by an underbar, $\underline{K}$.

Functionals shall be denoted with rectangular brackets for arguments, i.e. $\mathcal{F}_{[\phi]}$.

In this thesis we will regularly label momenta by a number, i.e. $\boldsymbol{k}_2, \boldsymbol{k}_4$. Following this, we introduce the following shorthand for integration over the Lorentz invariant measure,

$$\int_i = \int \frac{d^3 k_i}{(2\pi)^3} \ .$$

Chapter 2

Relativistic Kinetic Theory

2.1 The distribution function

Following the basic guiding principle of statistical physics, our goal is to study the behaviour of a macroscopic system (a model for the QGP) by a course grained description of the behaviour of its microscopic constituents (gluons). In this thesis our method of transforming the study of the latter into predictions for the former will be *kinetic theory*.

To this end, we categorize the system with the one-particle distribution function $f(t, \boldsymbol{x}, \boldsymbol{k})$, which counts the number of particles per phase space volume element $d^3x d^3k$ at a time t,

$$f(t, \boldsymbol{x}, \boldsymbol{k}) = \frac{dN(t)}{d^3x d^3k} \,.$$

Since both the total number of particles (N) and the phase space measure, for on-shell particles, ($d^3x d^3k$) are Lorentz invariant, f is too.

We can express macroscopic quantities in a manifestly covariant form by taking moments of the distribution function. Taking the first moment we define the *particle four-current*

$$J^\mu(\boldsymbol{x}) = \int \frac{d^3k}{(2\pi)^3} \frac{1}{E_k} k^\mu f(\boldsymbol{x}, \boldsymbol{k}) \,. \tag{2.1}$$

The time component, since $k^0 = E_k$, gives the *particle number density*

$$n(\boldsymbol{x}) = \int \frac{d^3k}{(2\pi)^3} f(\boldsymbol{x}, \boldsymbol{k}) \,, \tag{2.2}$$

while the spatial component gives the *particle number current*

$$\boldsymbol{j}(\boldsymbol{x}) = \int \frac{d^3k}{(2\pi)^3} \frac{\boldsymbol{k}}{E_k} f(\boldsymbol{x}, \boldsymbol{k}) = \int \frac{d^3k}{(2\pi)^3} \boldsymbol{v} f(\boldsymbol{x}, \boldsymbol{k}) \,. \tag{2.3}$$

From this, we introduce the *Eckart definition* of the fluid flow velocity

$$\boldsymbol{v}_{\mathrm{Eck}}(\boldsymbol{x}) := \frac{\boldsymbol{j}(\boldsymbol{x})}{n(\boldsymbol{x})} \,, \tag{2.4}$$

and the covariant fluid flow four-velocity

$$u^\mu_{\text{Eck}} = \gamma_{v_{\text{Eck}}} \begin{pmatrix} 1 \\ \boldsymbol{v}_{\text{Eck}} \end{pmatrix} = \frac{J^\mu}{\sqrt{J_\mu J^\mu}} \,. \tag{2.5}$$

Note that the local rest frame of the fluid is the one in which $u^\mu = (1, 0, 0, 0)$.

Taking the second moment of the distribution function we define the *energy-momentum tensor*

$$T^{\mu\nu}(\boldsymbol{x}) = T^{\nu\mu}(\boldsymbol{x}) = \int \frac{d^3k}{(2\pi)^3} \frac{k^\mu k^\nu}{E_k} f(\boldsymbol{x}, \boldsymbol{k}) \,, \tag{2.6}$$

which for $\mu = \nu = 0$ gives the energy density

$$\varepsilon(\boldsymbol{x}) := T^{00} = \int \frac{d^3k}{(2\pi)^3} E_k f(\boldsymbol{x}, \boldsymbol{k}) \,, \tag{2.7}$$

while T^{0i} gives the momentum density and T^{ij} the (Euclidean) stress tensor.

2.2 The Boltzmann equation

We shall study the behaviour of the distribution function under the Boltzmann Equation, which can be rigorously derived by truncating the Bogoliubov-Born-Green-Kirkwood-Yvon (BBGKY) hierarchy. For illustration purposes, we will choose rather to follow simple principles arrive at the correct form of the classical Boltzmann Equation [4].

Consider the "motion" of a phase space element $d^3x d^3k$ in the time interval $[t, t + \delta t]$. The number of particles in this phase space cell at time t is δN. At the later time $t = t + \delta t$, this phase space element will develop into another element $d^3x' d^3k'$ in which the number of contained particles is $\delta N' = f(t + \delta t, \boldsymbol{x}', \boldsymbol{k}')$. Assuming no particle interactions the phase space coordinates change as

$$\boldsymbol{x}' = \boldsymbol{x} + \boldsymbol{v}_x \delta t, \qquad \boldsymbol{k}' = \boldsymbol{k} + \boldsymbol{F} \delta t \,,$$

where $\boldsymbol{F}$ is an external force. If this force is conservative, by Louiville's Theorem [5] we have $d^3x d^3k = d^3x' d^3k'$. Therefore the consequent rate at which f is changed is

$$\begin{aligned} \frac{\delta N' - \delta N}{\delta t \, d^3x d^3k} &= \left[\partial_t + \boldsymbol{v}_x \cdot \nabla + \boldsymbol{F} \cdot \frac{\partial}{\partial \boldsymbol{k}} \right] f \\ &= \left[\partial_t + \boldsymbol{v}_\Gamma \cdot \boldsymbol{\nabla}_\Gamma \right] f =: \mathcal{D}_t f \,, \end{aligned} \tag{2.8}$$

where we've introduced the shorthand $\boldsymbol{\nabla}_\Gamma = (\boldsymbol{\nabla}_x, \boldsymbol{\nabla}_k)$, $\boldsymbol{v}_\Gamma = (\boldsymbol{v}_x, \boldsymbol{v}_k)$ and noted $\boldsymbol{v}_k = \partial_{\boldsymbol{x}} \mathcal{H} = \boldsymbol{F}$.

We recognize the term in brackets as the convective derivative $\mathcal{D}_t$, describing the rate at which phase space elements gain or lose particles through their free motion or in collisions.

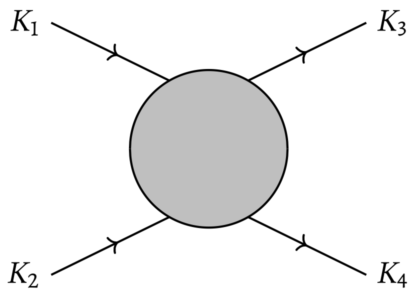

FIGURE 2.1: Convention for the labeling of external momenta $\{K_1, K_2\} \longrightarrow \{K_3, K_4\}$ for a generic $2 \longrightarrow 2$ scattering process.

This rate is given by the collision term $C_{[f]}$, a functional of the distribution function,

$$\mathcal{D}_t f = C_{[f]} \,. \tag{2.9}$$

For binary collisions (see Figure 2.1 for momenta labeling convention), under the assumption of *molecular chaos* [6] (also known as *Boltzmann's Stoßzahlansatz*), the collision term reads

$$\begin{aligned} C_{[f]} \coloneqq \int d^3k_2 d^3k_3 d^3k_4 \, W(\boldsymbol{k}_1, \boldsymbol{k}_2; \boldsymbol{k}_3, \boldsymbol{k}_4) \big[& f(t, \boldsymbol{x}_1, \boldsymbol{k}_1) f(t, \boldsymbol{x}_2, \boldsymbol{k}_2) \\ & - f(t, \boldsymbol{x}_3, \boldsymbol{k}_4) f(t, \boldsymbol{x}_3, \boldsymbol{k}_4) \big] \,, \end{aligned} \tag{2.10}$$

where $W(\boldsymbol{k}_1, \boldsymbol{k}_2; \boldsymbol{k}_3, \boldsymbol{k}_4)$ refers to the transition probability $\{\boldsymbol{k}_1, \boldsymbol{k}_2\} \longrightarrow \{\boldsymbol{k}_3, \boldsymbol{k}_4\}$, i.e. the probability that a collision between particles of momenta $\boldsymbol{k}_1$ and $\boldsymbol{k}_2$ will result in momenta $\boldsymbol{k}_3$ and $\boldsymbol{k}_4$. This non-linear integro-differential equation is known as the (classical) *Boltzmann Equation*.

As we shall be considering physical collisions, therefore ones obeying simple symmetry properties, it is worthwhile to point out the consequent restrictions this places on the transition probability. From conservation of momentum and energy, it follows that

$$W(\boldsymbol{k}_1, \boldsymbol{k}_2; \boldsymbol{k}_3, \boldsymbol{k}_4) \propto \delta^{(4)}(K_1 + K_2 - K_3 - K_4). \tag{2.11}$$

For exchanges that are invariant under time reversal, we must have

$$W(\boldsymbol{k}_1, \boldsymbol{k}_2; \boldsymbol{k}_3, \boldsymbol{k}_4) = W(-\boldsymbol{k}_3, -\boldsymbol{k}_4; -\boldsymbol{k}_1, -\boldsymbol{k}_2) \,, \tag{2.12a}$$

and for those that are parity invariant we must have

$$W(\boldsymbol{k}_1, \boldsymbol{k}_2; \boldsymbol{k}_3, \boldsymbol{k}_4) = W(-\boldsymbol{k}_1, -\boldsymbol{k}_2; -\boldsymbol{k}_3, -\boldsymbol{k}_4) \,. \tag{2.12b}$$

In combination, this yields the important relation of invariance under particle exchange

$$W(\boldsymbol{k}_1, \boldsymbol{k}_2; \boldsymbol{k}_3, \boldsymbol{k}_4) = W(\boldsymbol{k}_3, \boldsymbol{k}_4; \boldsymbol{k}_1, \boldsymbol{k}_2)\,. \tag{2.13}$$

More relevant to our study is the generalization of the collision term in Eq. (2.10) to include quantum statistics, allowing the study of gasses of quantum particles [7, 8]. Identifying the transition probability with the square of the matrix element of the interaction, we write

$$C_{[f]} := \frac{1}{2E} \int d\Gamma\, |\mathcal{M}|^2 \mathcal{F}_{[f]}\,, \tag{2.14}$$

where $|\mathcal{M}|^2$ is averaged over the incoming particles' spin states and summed over the outgoing particles' spin states. Here two-body phase space is abbreviated as

$$\int d\Gamma := \int_{234} \frac{(2\pi)^4}{8E_2E_3E_4} \delta^{(4)}(K_1 + K_2 - K_3 - K_4)\,, \tag{2.15}$$

having used $\int_i = \int d^3k_i/(2\pi)^3$ as shorthand for the momentum integrals. The gain and loss terms are represented in the *distribution functional*

$$\mathcal{F}_{[f]} := \bar{f}_1 \bar{f}_2 f_3 f_4 - f_1 f_2 \bar{f}_3 \bar{f}_4\,, \tag{2.16}$$

where the subscript has been used as shorthand for the momentum argument, $f_i = f(\boldsymbol{k}_i)$ and the bar notation $\bar{f} = 1 \pm f$ codes the Bose-enhancement of Bosons (upper sign) and the Pauli-blocking of Fermions (lower sign).

2.2.1 Collisional invariants

A key strength of kinetic theory is the ability to connect the microscopic details of a system's collisions (as represented in the collision term (2.14)) with its macroscopic properties. Of particular interest to us are the properties that are left unchanged through the collisions — conserved quantities.

Consider a function $\phi(\boldsymbol{x}, \boldsymbol{k})$ defined over the single particle phase space, and the quantity derived from averaging it over momentum space, $\Phi(t, \boldsymbol{x}) := \int_k \phi(\boldsymbol{x}, \boldsymbol{k}) f(t, \boldsymbol{x}, \boldsymbol{k})$. To study the evolution of this quantity, we take the time derivative

$$\begin{aligned}\partial_t \Phi &= \int_{\boldsymbol{k}} \phi \, \frac{\partial f}{\partial t} \\ &= \int_{\boldsymbol{k}} \phi \{ C_{[f]} - (\boldsymbol{v}_\Gamma \cdot \boldsymbol{\nabla}_\Gamma) f \} \\ &= \int_{\boldsymbol{k}} \left\{ \phi \, C_{[f]} - f \left(\frac{\partial \boldsymbol{x}}{\partial t} \cdot \frac{\partial \phi}{\partial \boldsymbol{x}} + \frac{\partial \boldsymbol{k}}{\partial t} \cdot \frac{\partial \phi}{\partial \boldsymbol{k}} \right) \right\} \\ &= \int_{\boldsymbol{k}} \left\{ \phi \, C_{[f]} - f \frac{d\phi}{dt} \right\} .\end{aligned} \tag{2.17}$$

As $d\phi/dt = 0$, the evolution is fully determined by the collision term

$$\partial_t \Phi(t, \boldsymbol{x}) = \int_{\boldsymbol{k}} \phi(\boldsymbol{x}, \boldsymbol{k}) \, C_{[f(t,\boldsymbol{x},\boldsymbol{k})]} \, . \tag{2.18}$$

Conserved quantities are those that satisfy $\partial_t \Phi(t, \boldsymbol{x}) = 0$. The functions $\phi(\boldsymbol{x}, \boldsymbol{k})$ that when multiplied by the collision term and integrated over momentum return a vanishing result are called *collisional invariants*. For the integral to vanish, we must have

$$\int_{\boldsymbol{k}} \phi(\boldsymbol{x}, \boldsymbol{k}) \, C_{[f(t,\boldsymbol{x},\boldsymbol{k})]} = \int_{\boldsymbol{k}} \int d\Gamma \, \phi(\boldsymbol{x}, \boldsymbol{k}) W(\boldsymbol{k}_1, \boldsymbol{k}_2; \boldsymbol{k}_3, \boldsymbol{k}_4) \mathcal{F}_{[f(t,\boldsymbol{x},\boldsymbol{k})]} = 0 \, . \tag{2.19}$$

Making use of the symmetry properties of the transition probability, as given in Equations (2.12) and (2.13), we can arrive at the simple property

$$\phi(\boldsymbol{x}, \boldsymbol{k}_1) + \phi(\boldsymbol{x}, \boldsymbol{k}_2) = \phi(\boldsymbol{x}, \boldsymbol{k}_3) + \phi(\boldsymbol{x}, \boldsymbol{k}_4) \, . \tag{2.20}$$

The Boltzmann equation permits exactly five collisional invariants [9]; $\phi = 1$ (particle number conservation) and $\phi = K^\mu$ (energy-momentum conservation).

2.2.2 Equilibriation

We will now show that the Boltzmann equation drives the distribution function towards equilibrium, a function $f^{\text{eq}}(t, \boldsymbol{x}, \boldsymbol{k})$ for which $C_{[f^{\text{eq}}]} = 0$, by introducing Boltzmann's *H-Theorem*. For simplicity's sake, we assume spatial homogoneity of the distribution function.

For the collision term to vanish, we must have a balance between the gain and loss terms of the distribution functional $\mathcal{F}_{[f]}$ (2.16),

$$\bar{f}_1 \bar{f}_2 f_3 f_4 = f_1 f_2 \bar{f}_3 \bar{f}_4 \, , \tag{2.21}$$

or, equivalently,

$$\log\left(\frac{f_1}{\bar{f}_1}\right) + \log\left(\frac{f_2}{\bar{f}_2}\right) = \log\left(\frac{f_3}{\bar{f}_3}\right) + \log\left(\frac{f_4}{\bar{f}_4}\right). \tag{2.22}$$

Noting the similarity between Equations (2.22) and (2.20), read the former as a statement that sum of the $\log(f/\bar{f})$ must be conserved in the collision. Thus the logarithm must be a function of the five collisional invariants,

$$\log\left(\frac{f(\boldsymbol{k})}{\bar{f}(\boldsymbol{k})}\right) = \left(\mu - E + \boldsymbol{u}\cdot\boldsymbol{k}\right)/T\,, \tag{2.23}$$

giving us the familiar Bose-Einstein distribution function

$$f^{\text{eq}}(\boldsymbol{k}) = \frac{1}{\exp[(E - \mu - \boldsymbol{u}\cdot\boldsymbol{k})/T] - 1}\,, \tag{2.24}$$

where the parameters μ and T represent the chemical potential and inverse temperature respectively.

The assumption of molecular chaos (colliding particles' momenta are uncorrelated before the collision) is enough to introduce a clear flow of time in the behaviour of a system under the Boltzmann equation. Subject to dynamics as given by the collision term (2.14), an initial distribution function will evolve towards its equilibrium. To see this we will show that the solutions to the Boltzmann equation obey the second law of thermodynamics (entropy never decreases), thereby giving a clear arrow of time to their evolution.

In a system of bosons, each quantum state can contain an arbitrary number of particles, but each of these particles are indistinguishable. Thus if we have N_i particles contained within a phase space element $d^3x d^3k$ to distribute these over the G_i single particle states in the same phase space element, the number of ways to do this is [6]

$$\Omega_i = \begin{pmatrix} G_i + N_i - 1 \\ N_i \end{pmatrix} = \frac{(G_i - N_i - 1)!}{(G_i - 1)!N_i!}\,. \tag{2.25}$$

Then using Stirling's approximation we calculate the total entropy of a system with a given distribution of N_i particles as

$$S = \sum_i \Big[(G_i + N_i)\log(G_i + N_i) - N_i \log(N_i) - G_i \log(G_i)\Big]\,, \tag{2.26}$$

or, introducing the mean occupation number $f_i = N_i/G_i$ of the i-th phase space cell,

$$\begin{aligned} S &= -\sum_i G_i\Big[f_i \log(f_i) - (1 + f_i)\log(1 + f_i)\Big] \\ &= -\frac{1}{(2\pi)^3}\int d^3x \int d^3k \Big[f\log(f) - \bar{f}\log(\bar{f})\Big]\,. \end{aligned} \tag{2.27}$$

From this, we define the relativistic entropy density four-current as

$$s^\mu(\boldsymbol{x}) = -\int_{\boldsymbol{k}} k^\mu \Big(f(\boldsymbol{x},\boldsymbol{k}) \log(f(\boldsymbol{x},\boldsymbol{k})) - \bar{f}(\boldsymbol{x},\boldsymbol{k}) \log(\bar{f}(\boldsymbol{x},\boldsymbol{k})) \Big) \tag{2.28}$$

allowing us to state the second law of thermodynamics, as generalized to a relativistic system,

$$\partial_\mu s^\mu \geq 0\,. \tag{2.29}$$

We can show that the equilibrium distribution (2.24) does indeed maximize the entropy through the method of Lagrange multipliers.

That the solutions of the Boltzmann equation do indeed obey Equation (2.29) was shown by Boltzmann through his *H-theorem*

$$H = -S \leq 0\,. \tag{2.30}$$

2.3 Bose-Einstein condensation

Under the Boltzmann equation, an initial distribution function evolves asymptotically to equilibrium. This equilibrium distribution function (2.24) (and consequently its energy and number density) is fully categorized by the two equilibrium parameters $\{\mu, T\}$, or equivalently $\{\nu := -\mu/T, T\}$

$$\varepsilon_{\text{eq}}(T,\nu) = 3T^4 \mathsf{L}_4(\nu) \tag{2.31a}$$

$$n_{\text{eq}}(T,\nu) = T^3 \mathsf{L}_3(\nu)\,, \tag{2.31b}$$

where we've introduced the shorthand $\mathsf{L}_n(x) := \text{Li}_n(\exp(x))/\pi^2$, and $\text{Li}_n(x)$ is the polylogarithm of order n. Through conservation laws these equilibrium parameters are fully determined by the initial distribution's number and energy density, which we take as fixed

$$\varepsilon_{\text{eq}}(T,\nu) \stackrel{!}{=} \underline{\varepsilon_{\text{in}}} \tag{2.32a}$$

$$n_{\text{eq}}(T,\nu) \stackrel{!}{=} \underline{n_{\text{in}}}\,. \tag{2.32b}$$

Although we are guaranteed a solution to the above system of equations, some solutions may not be physically realizable by having a non-negative chemical potential value corresponding to a distribution function that is not strictly non-negative.

We will now look closer at the solutions of Equations (2.32a, 2.32b). This system of equations define two lines in the ν-T plane, with gradients

$$\partial_T \left[\varepsilon_{\text{eq}}(T,\nu) \right] = \partial_T \varepsilon_{\text{eq}}(T,\nu) + \partial_\nu \varepsilon_{\text{eq}}(T,\nu) \partial_T \nu = 0$$

$$\implies \partial_T \nu_\varepsilon = \frac{4}{T}\frac{\mathrm{L}_4(\nu)}{\mathrm{L}_3(\nu)}, \tag{2.33a}$$

and

$$\partial_T\left[n_{\rm eq}(T,\nu)\right] = \partial_T n_{\rm eq}(T,\nu) + \partial_\nu n_{\rm eq}(T,\nu)\partial_T\nu = 0$$
$$\implies \partial_T \nu_n = \frac{3}{T}\frac{\mathrm{L}_3(\nu)}{\mathrm{L}_2(\nu)}. \tag{2.33b}$$

It is easy to numerically verify that

$$4\frac{\mathrm{L}_4(\nu)}{\mathrm{L}_3(\nu)} > 3\frac{\mathrm{L}_3(\nu)}{\mathrm{L}_2(\nu)},$$

for all values of ν, thus ensuring $\partial_T\nu_\varepsilon > \partial_T\nu_n$ and allowing us identify a *unique* "critical" situation in which the two lines described by Equations (2.32a, 2.32b) intersect at $\nu = 0$. With this, we classify our system as either *underpopulated* (intersection at $\nu > 0$), *critically populated* (intersection at $\nu = 0$) or *overpopulated* (intersection at $\nu < 0$).

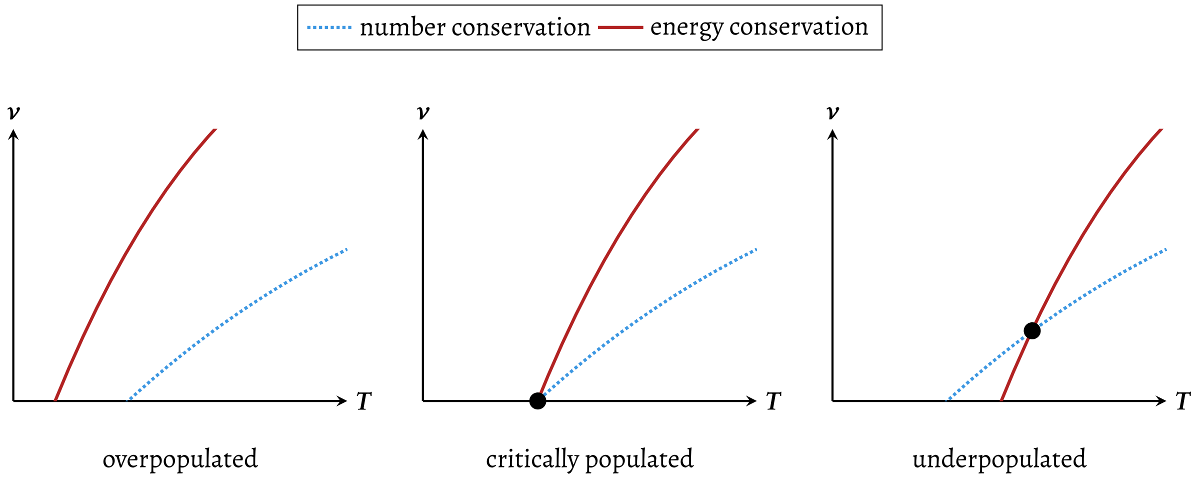

FIGURE 2.2: Stylized depiction of the ν-T parameter space for overpopulated, critically populated and underpopulated systems.

Overpopulated systems are those in which the total particle density is greater than that of the excited states of the Bose-Einstein distribution, thereby forcing the "excess" constituents into all occupying the lowest energy state, with $\boldsymbol{k} = 0$. This macroscopic occupation of the single one-particle state is known as *Bose-Einstein condensation*. Practically, for our book-keeping purposes, this is achieved by modifying the equilibrium distribution (2.24) to

$$f^{\rm eq}(\boldsymbol{k}) = \frac{1}{\exp([E - \boldsymbol{u}\cdot\boldsymbol{k}]/T) - 1} + (2\pi)^3 n_c \delta^{(3)}(\boldsymbol{k}), \tag{2.34}$$

still described fully by two equilibrium parameters, n_c (the number of particles in the condensate) now replacing μ in the parametrization.

Bose-Einstein condensation has been successfully observed in many systems [10–14], but has not yet been observed in a system of gluons. However, as the Color Glass Condensate (CGC) model predicts the saturation of gluon densities in high energy collisions [15], researchers have proposed the possibility of the suppression of number-changing collisions and a formation of a transient gluon condensate in the evolution of the quark-gluon plasma [16–18].

Chapter 3

Solving the Boltzmann Equation

3.1 Illustrating the two-body phase space

In this thesis we use a system of spatially homogeneous gluons, isotropically distributed in momentum space, to model the far more complicated quark-gluon plasma (QGP). In doing so we hope to capture some salient properties of the evolution of the QGP while allowing sufficient simplicity in some aspects of the evolution to compensate for more thorough investigation of others. In this vein we choose to include in our analysis the effect of the coupling between our gluons and their thermal fluctuations.

At finite temperature otherwise massless fields acquire a *thermal mass* [19]

$$m_{\text{th}} \sim \lambda T \,, \tag{3.1}$$

where λ is the coupling constant. This thermal mass appears as a modification to the dispersion relation of the propagating field. In more complex theories (QCD certainly being one of them) the thermal mass is typically a function of the frequency and momentum of the propagation, but the temperature scaling (3.1) remains the same. This effective mass will be treated as constant for the remainder of this work, referred to simply as m. Beyond the acquisition of a thermal mass, fields also encounter screening effects due to the presence of the thermal medium. We will revisit this in Chapter 5.

Before we're able to tackle the collision term, we need to have a good understanding of the two body phase space as given by Equation (2.15). To do so, we introduce the *Mandelstam invariants*

$$\begin{aligned} s &= (K_1 + K_2)^2 = (K_3 + K_4)^2 \,, \\ t &= (K_1 - K_3)^2 = (K_2 - K_4)^2 \,, \\ u &= (K_1 - K_4)^2 = (K_2 - K_3)^2 \,. \end{aligned} \tag{3.2}$$

From energy-momentum conservation and the on-shell conditions ($K_i^2 = m^2$) we may conclude that these invariants are not independent of each other,

$$\begin{aligned} s + t + u &= 6m^2 + 2(K_1 \cdot K_2 - K_1 \cdot K_3 - K_1 \cdot K_4) \\ &= 6m^2 + 2K_1 \cdot (K_2 - K_3 - K_4) = 4m^2 \,. \end{aligned} \tag{3.3}$$

Thus, we have only two independent Mandelstam invariants with which to categorize a collision (in this thesis, we will typically use s and t). Imbuing these invariants with physical meaning, we associate s with the total energy of the collision (it is indeed the square of the energies of the incoming particles in the center of mass frame) and t with the momentum transfer of the collision (closely related to the scattering angle in the center of mass frame).

We now simplify the integration over the collision phase space (2.15) as an integral over the Mandelstam invariants s, t and and an integral over the outgoing energies E_3, E_4. The details of the calculation can be found in Appendix A, we quote here a sketch of the result:

$$\int d\Gamma \left\{ \dots \right\} = \iint_{\mathcal{R}} dE_3 dE_4 \, \mathcal{I}_{[\{\dots\}]} \,, \tag{3.4}$$

where

$$\mathcal{I}_{[\{\dots\}]} = \int_{s_-}^{s^+} ds \int_{t_-}^{t^+} dt \frac{1}{\sqrt{Q}} \left\{ \dots \right\}, \tag{3.5}$$

with Q a quadratic function of t, the coefficients of which, along with the bounds $s_\pm, t_\pm$, being functions of the remaining integration variables. The "Mandelstam integral" (3.5) will be discussed in more detail in Appendix D when we look at specific forms of the collision term. For now we focus our attention on the E_3E_4 phase space in Equation (3.4).

In aid of the later discritization of the phase space we introduce an ultraviolet (UV) cutoff Λ_{UV}, such that $E_i \leq \Lambda_{\text{UV}}$. A quick dimensional analysis of the collision term (2.14) confirms that, noting that the distribution functional $\mathcal{F}$ consists only of terms cubic and quadratic in the distribution f, for distributions $f(k)$ that drop faster than $1/k$ at large k the collision term is UV finite. Thus, assuming a sufficiently large value of Λ_{UV} is chosen we expect no pathological behaviour of the Boltzmann equation (unlike, as discussed in [20, 21], in the case of its classical approximation). With this our E_3E_4 phase space is fully determined by the restrictions $m \leq E_i \leq \Lambda_{\text{UV}}$, and is depicted in Figure 3.1.

3.2 Capturing condensate dynamics

In this section we will modify the Boltzmann equation under the presence of a Bose-Einstein condensate with the goal of explicitly detailing the evolution of the condensate. To do this we

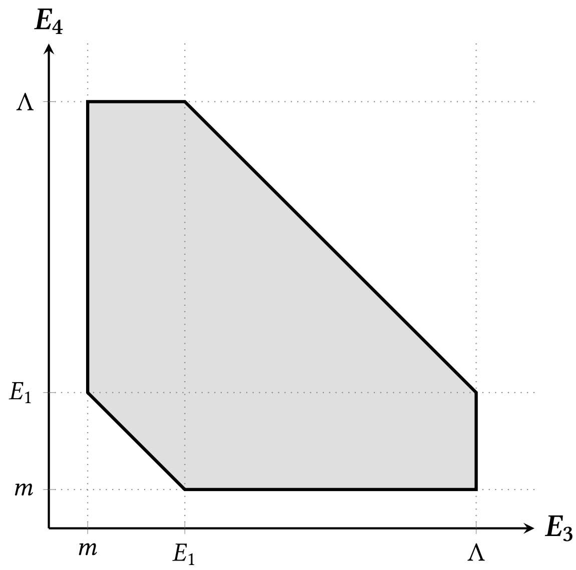

FIGURE 3.1: Integration phase space for (3.4) over the variables E_3 and E_4. The bottom and top diagonal boundaries correspond to $\underline{E}_2 = m$ and $\underline{E}_2 = \Lambda_{\mathrm{UV}}$ respectively.

include in the distribution a condensate term

$$f \rightarrow f(\boldsymbol{k}) + n_c(2\pi)^3\delta^{(3)}(\boldsymbol{k}), \tag{3.6}$$

where $f(\boldsymbol{k})$ is understood as the *regular* part of the distribution, finite near the origin [22]. With this modification, the distribution functional becomes

$$\mathcal{F}_{[f]} \rightarrow \mathcal{F}_{[f]} + n_c(2\pi)^3\Big\{\delta^{(3)}(\boldsymbol{k}_1)\mathcal{F}^{c234}_{[f]} + \delta^{(3)}(\boldsymbol{k}_2)\mathcal{F}^{1c34}_{[f]} + \delta^{(3)}(\boldsymbol{k}_3)\mathcal{F}^{12c4}_{[f]} + \delta^{(3)}(\boldsymbol{k}_4)\mathcal{F}^{123c}_{[f]}\Big\} + \mathcal{O}(n_c^2), \tag{3.7}$$

where

$$\mathcal{F}^{c234}_{[f]} = \bar{f}_2 f_3 f_4 - f_2 \bar{f}_3 \bar{f}_4, \tag{3.8a}$$

$$\mathcal{F}^{1c34}_{[f]} = \bar{f}_1 f_3 f_4 - f_1 \bar{f}_3 \bar{f}_4, \tag{3.8b}$$

$$\mathcal{F}^{12c4}_{[f]} = \bar{f}_1 \bar{f}_2 f_4 - f_1 f_2 \bar{f}_4, \tag{3.8c}$$

$$\mathcal{F}^{123c}_{[f]} = \bar{f}_1 \bar{f}_2 f_3 - f_1 f_2 \bar{f}_3. \tag{3.8d}$$

Note here that we've excluded the terms quadratic and higher in n_c as these terms all vanish when substituting Equation (3.6) into the collision term.

We now integrate the Boltzmann equation over an infinitesimal sphere in $\boldsymbol{k}_1$. Doing so allows us to get the following two coupled equations

$$\partial_t f = C_{[f]} + n_c \left\{ C^{\text{out}}_{[f]} + 2C^{\text{in}}_{[f]} \right\} , \tag{3.9a}$$

and

$$\partial_t n_c = n_c \mathcal{R}_{c[f]} \tag{3.9b}$$

Here we've introduced the shorthand

$$C^{\text{out}}_{[f]}(\boldsymbol{k}_1) := \frac{1}{16mE_1} \int_{34} \frac{(2\pi)^4}{E_3 E_4} \mathcal{F}^{1c34}_{[f]} \left(\delta^{(4)}(K_1 + K_2 + K_3 + K_4) |\mathcal{M}|^2 \right) \Big|_{\boldsymbol{k}_2 = 0} , \tag{3.10a}$$

$$C^{\text{in}}_{[f]}(\boldsymbol{k}_1) := \frac{1}{16mE_1} \int_{24} \frac{(2\pi)^4}{E_2 E_4} \mathcal{F}^{12c4}_{[f]} \left(\delta^{(4)}(K_1 + K_2 + K_3 + K_4) |\mathcal{M}|^2 \right) \Big|_{\boldsymbol{k}_3 = 0} , \tag{3.10b}$$

and

$$\mathcal{R}_{c[f]} := \frac{1}{2m} \int d\Gamma (2\pi)^4 \mathcal{F}^{c234}_{[f]} \left(\delta^{(4)}(K_1 + K_2 + K_3 + K_4) |\mathcal{M}|^2 \right) \Big|_{\boldsymbol{k}_1 = 0} . \tag{3.10c}$$

Note the relative factor of two between the two terms in the bracket of (3.9a) representing the two available options of scattering into the condensate ($\boldsymbol{k}_3 = 0$ or $\boldsymbol{k}_4 = 0$).

With Equations (3.9) the conservation laws read

$$\text{number conservation:} \qquad \mathcal{R}_{c[f]} + \int_{\boldsymbol{k}} \left(C^{\text{in}}_{[f]} + 2C^{\text{out}}_{[f]} \right) = 0 , \tag{3.11a}$$

$$\text{energy conservation:} \qquad m\mathcal{R}_{c[f]} + \int_{\boldsymbol{k}} E_k \left(C^{\text{in}}_{[f]} + 2C^{\text{out}}_{[f]} \right) = 0 , \tag{3.11b}$$

$$\text{momentum conservation:} \qquad \int_{\boldsymbol{k}} \boldsymbol{k} \left(C^{\text{in}}_{[f]} + 2C^{\text{out}}_{[f]} \right) = 0 . \tag{3.11c}$$

3.3 Numerically solving the Boltzmann equation

3.3.1 Discretization

In order to have access to the time evolution of the distribution function, we will numerically solve the Boltzmann equation. To do so we will need to recast the Boltzmann equation into a discrete form in both time and momentum (recall that we've made the simplifying assumption of spatial homogeneity). The bulk of our numerical effort will be taken in evaluating the collision term which, through our simplification of the momentum phase space as discussed in Section 3.1, we've managed to reduce from a ninefold integral to a fourfold integral (3.4). In chapters that follow we will look at the Mandelstam integral (3.5) in more detail and show that for interesting classes of matrix element $\mathcal{M}$ we can derive closed form expressions for $\mathcal{I}_{\mathcal{M}}$. Thus, in this section we will focus on the necessary discretization of momentum space.

As we've seen in Subsection 2.3, conservation of number and energy density determine the equilibrium of a given initial distribution by setting the equilibrium parameters. Thus, special care must be taken through the evolution to satisfy these conservation laws with high accuracy. This is of particular importance near the vicinity of Bose-Einstein condensation, where the system very suddenly picks up a macroscopic number of particles in the condensate. We will be using a discretization scheme that allows for the conservation laws to be satisfied exactly (following [20]), the details of which can be found in Appendix B.

As it requires an equidistant grid, in using this scheme we make the trade-off between exact conservation and grid efficiency. This is important to note because in its discretized form, the momentum space that makes up the domain of the distribution function necessarily has a smallest nonzero momentum k_δ — an artificial soft scale introduced into the problem. This smallest nonzero momentum plays the role of an inverse size of the system, thereby subtly breaking our assumption of spatial homogeneity. We shall see that this has the consequence of making the onset of condensation no longer a true discontinuous phase transition, but rather a sudden (but not immediate) transition. We can lessen this effect by sending $k_\delta \longrightarrow 0$. For an equidistant grid this corresponds to sending $N \longrightarrow \infty$, a very tall order given that an integration of E_3, E_4 phase space as in (3.4) scales like N^2 therefore making an overall evolution step scale as N^3. Were we to have the freedom of an irregular grid, we could devise one that clusters points in numerically relevant areas allowing us to have small values of k_δ for relatively smaller N.

To capture the extreme dynamics around the onset of condensation we use an adaptive timestep method to iterate through the evolution of the distribution function and its condensate. In particular, we use a Runge-Kutta-Fehlberg method of mixed order two and three, *RKF2(3)* [23].

3.3.2 Initial condition

As a rough model for the initial conditions for a quark-gluon-like evolution, we take inspiration from the Colour Glass Condensate (CGC) model and study distributions that are large for energy below some characteristic scale Q and negligible above Q,

$$f(E) = \chi\,\Theta(Q - E)\,. \tag{3.12}$$

Note that Q is not a true scale of the system as we can simply express all dimensionful quantities in units of Q; we will set $Q = 1$ for the remainder of this work. For numerical purposes we wish to "smooth out" the discontinuous Θ-function, leading us to rather consider the family of initial conditions

$$f_{\text{in}}(E) := \frac{\chi}{\exp[(E-1)/\sigma]+1}\,. \tag{3.13}$$

Algorithm 1: RKF2(3)

input : initial condition (t_i, x_i); tolerance TOL, initial time step Δ_t
output: successive iteration (t_{i+1}, x_{i+1})

set FLAG = false

while *FLAG = false* **do**
  set $y_1 = f(x_i)$
  set $y_2 = f(x_i + \Delta_t y_1)$
  set $y_3 = f(x_i + \Delta_t (y_1 + y_2)/4)$
  set $\epsilon = \Delta_t (y_1 + y_2 - 2y_3)/3$
  if $\epsilon \leq TOL$ **then**
    set FLAG = true
  else
    set $\Delta_t = 0.9\Delta_t (\mathrm{TOL}/\epsilon)^{1/3}$

set $\Delta_x = \Delta_t (y_1 + y_2 + 4y_3)/6$
return $(t + \Delta, x + \Delta_x)$

FIGURE 3.2: Simplified pseudocode of a Runge-Kutta-Fehlberg algorithm for the differential equation $\dot{x} = f(x(t))$.

Here σ plays the role of smoothing the discontinuity, smaller values of σ result in "sharper" corners (see Figure 3.3).

Initial conditions of the form (3.13) have closed form number and energy density expressions,

$$n_{\mathrm{in}}(\chi, \sigma) = -\frac{\chi\sigma^3}{\pi^2}\mathrm{Li}_3(-e^{1/\sigma}), \tag{3.14a}$$

$$\varepsilon_{\mathrm{in}}(\chi, \sigma) = -\frac{3\chi\sigma^4}{\pi^2}\mathrm{Li}_4(-e^{1/\sigma}). \tag{3.14b}$$

This allows us to, in principle, exactly determine the equilibrium parameters $\{\nu, T\}$ as a function of the initial condition parameters $\{\chi, \sigma\}$. In practice however, both our initial condition and equilibrium distribution will be discretized on our energy grid meaning these analytical relationships can be held only as approximations that improve with increasing density of the grid. That we can, as in Section 2.3, define a unique critical equilibrium solution and consequently uniquely define the under- and overpopulated regimes is proved in Appendix C.

From (3.9b), we see that our initial number of condensate particles must be non-zero in order for us to attempt capturing the macroscopic dynamics further in the evolution. We shall see that the exact value of $n_c(t = 0)$ chosen does not greatly effect the evolution of the system, as long as $n_c(t = 0)$ is negligible compared to the regular particle density (c.f. Figure 4.4).

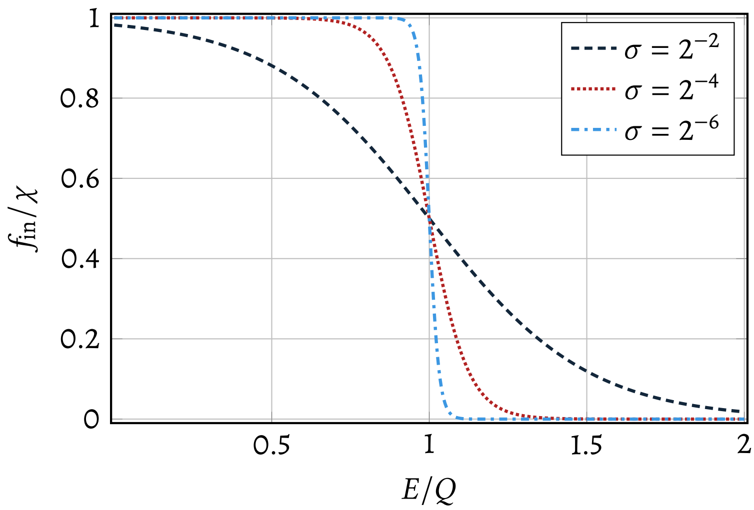

FIGURE 3.3: Initial condition (3.13) showing effect the value of σ has "shoulder" steepness.

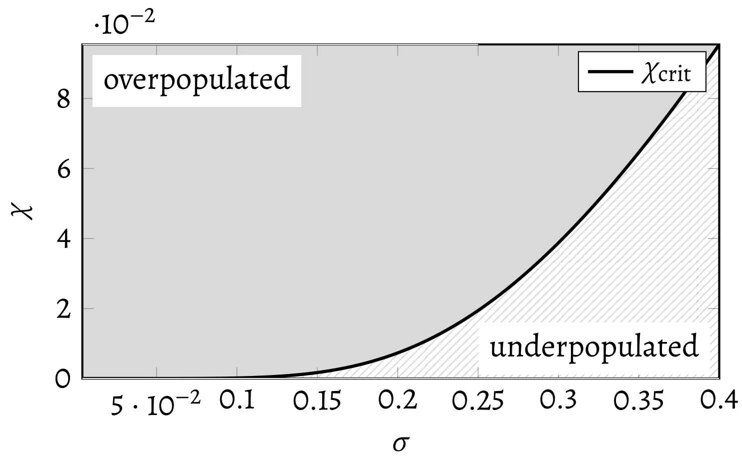

FIGURE 3.4: Initial condition parameter space, showing the (σ, χ) regions for which the system is underpopulated (hashed area), critically populated (solid line) and overpopulated (gray area).

Chapter 4

Toy Model: Scalar Theory

4.1 Simplifying the collision term

In this section we study the Boltzmann equation under scalar interactions. We show that our phase space decomposition and simplification (as discussed in Section 3.1) results in the known form of this collision term. Furthermore, we show that our numerical method (as discussed in Section 3.3) reproduces known results for the evolution of the distribution function and its condensate.

Under scalar interactions $|\mathcal{M}|^2 = \lambda^2$, using (3.4), the regular collision term is

$$C_{[f]} = \frac{1}{32(2\pi)^4 E_1 k_1} \iint_{\mathcal{R}} dE_3 dE_4\, \mathcal{F}_{[f]} \mathcal{K}_\lambda\,, \tag{4.1}$$

with

$$\mathcal{K}_\lambda = 2\lambda^2 \int_{s_-}^{s_+} ds \int_{t_-}^{t_+} dt \frac{1}{\sqrt{Q}}\,, \tag{4.2}$$

where Q and the Mandelstam integration limits $s_\pm$, $t_\pm$ are defined and discussed in Appendix A.

Recalling that Q can be expressed as a quadratic function in t with coefficients functions of the remaining integration variables (defined in Equation (A.11)), we evaluate the innermost integral

$$\int_{t_-}^{t_+} dt \frac{1}{\sqrt{Q}} = \int_{t_-}^{t_+} dt \frac{1}{\sqrt{a_t t^2 + b_t t + c_t}} = \frac{\pi}{\sqrt{-a_t}} = \frac{\pi}{\sqrt{(E_3+E_4)^2 - s}}\,, \tag{4.3}$$

where we've used that $t_\pm$ are the roots of $Q(t)$. Now, the integral over s is elementary

$$\begin{aligned} \int_{s_-}^{s_+} ds \frac{\pi}{\sqrt{(E_3+E_4)^2 - s}} &= \left[-2\pi\sqrt{(E_3+E_4)^2 - s} \right]_{s_-}^{s_+} \\ &= 2\pi \begin{cases} \min(k, \underline{k}_2) & \text{if } E_1\underline{E}_2 < E_3E_4 \\ \min(k_3, k_4) & \text{if } E_1\underline{E}_2 \geq E_3E_4 \end{cases}\,. \end{aligned} \tag{4.4}$$

Thus, we have

$$\mathcal{K}_\lambda = 4\pi\lambda^2 \min(k_1, \underline{k}_2, k_3, k_4)\,, \tag{4.5}$$

and

$$C_{[f]} = \frac{\lambda^2}{128\pi^3 E_1 k_1} \iint_{\mathcal{R}} dE_3 dE_4 \min(k_1, \underline{k}_2, k_3, k_4) \mathcal{F}_{[f]} \, . \tag{4.6}$$

This reproduces the result derived in [20] (Appendix B) and in the relativistic limit it reproduces the result derived in [24] (Appendix A).

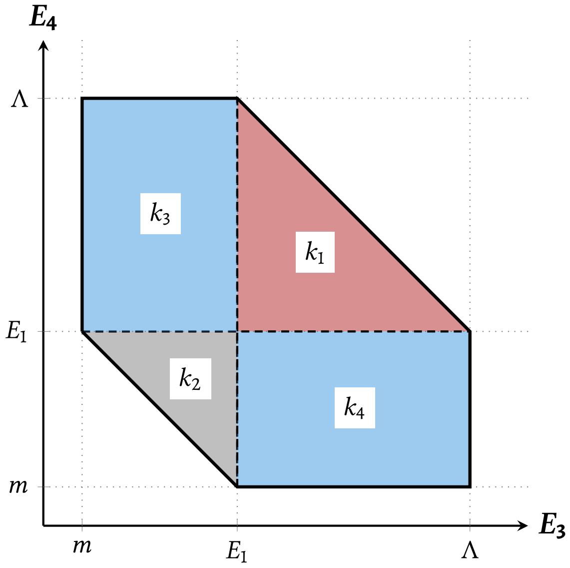

FIGURE 4.1: Integration phase space for (4.6) over the variables E_3 and E_4. The labels within the regions correspond to the value of $\mathcal{K}_\lambda \sim \min(k_1, \underline{k}_2, k_3, k_4)$ in that subdomain.

4.2 Soft momentum behaviour

A defining characteristic of the expected Bose-Einstein equilibrium distribution is the behaviour at soft momenta: $f^{\text{eq}}|_{k\to 0} \sim 1/E$. In this section, we'll look at the small-k behaviour of the collision term (4.6) under different forms of the distribution function. For simplicity's sake we will neglect the existence of a mass in this discussion, but through a more cumbersome set of calculations one can confirm that the results of this section generalize to the case $E \neq k$.

We begin by studying a fully regular, well-behaved, initial condition. For small k_1 the phase space becomes dominated by region ④ (see Fig. 4.2). In the limit $k \to 0$ the integration of an IR-regular distribution functional over the regions ①, ② and ③ produce a vanishingly small contribution to the collision term. In region ④, $\mathcal{K}_\lambda \sim k_1$, and we get

$$C(\boldsymbol{k}_1) \underset{k_1\to 0}{\sim} \frac{1}{k_1} \iint_{④} dk_3 dk_4 \left(\frac{k_1}{k_1}\right) \mathcal{F}_{[f]} \sim \frac{1}{k_1} \, , \tag{4.7}$$

where we've noted that for the regular integrand, the integration produces a finite result. Curiously, we see that in the evolution of a distribution function it immediately picks up an IR

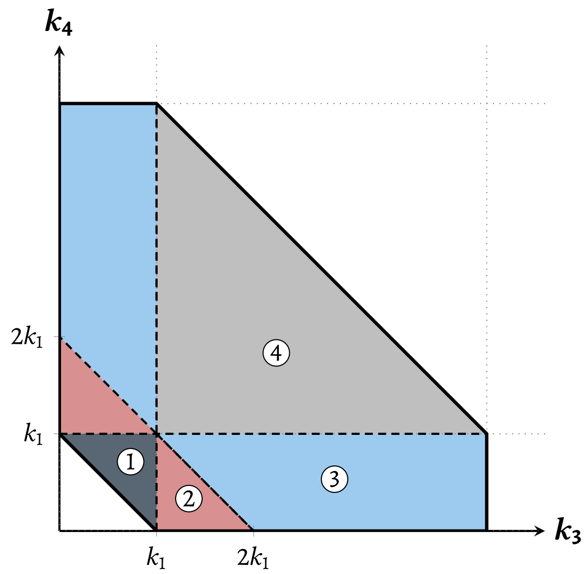

FIGURE 4.2: Integration region for (4.6) in the limit of small-k. Four regions are differentiated: ① in which k_1, $\underline{k}_2$, k_3 and k_4 are small, ② in which k_1, $\underline{k}_2$ and k_4 are small, ③ in which k_1 and k_4 are small and ④ in which only k_1 is small.

divergent component. Numerically this component is tempered by the timestep of the evolution, becoming a "suppressed" $\Delta t/k_1$ contribution.

Now we consider the evolution at some time other than $t = 0$, in which the distribution contains the IR divergent contribution $f \to f(k_1) + a/k_1$ $(a \in \mathbb{R})$. We wish to confirm that the leading behaviour remains $1/k_1$. Note that the dominant contributions to the integrand come from regions ①, ② and ③ in which one or more of the momenta $\underline{k}_2$, k_3 and k_4 become small. Note that we're free to consider only these regions and not their corresponding mirrored regions due to the k_3-k_4 symmetry of the integral. Looking at the forms of these integrals we can observe the imperfect balancing between factors of k_1 from the area of a region with factors of $1/k_1$ from the distribution functional $\mathcal{F}_{[f]}$ leading to a resultant $1/k_1$ behaviour. To illustrate this we'll study the dominant divergent contribution to the integrand in each of these regions and show that the resulting integral produces at most a $1/k_1$ divergence.

Proceeding in reverse order, region ③ has $k_4 \lesssim k_1$ making the dominant contribution to the functional $\mathcal{F}_{[f]}$ come from f_4,

$$\mathcal{F}_{[f]} \underset{k_4 \to 0}{\sim} \frac{1}{k_4} \left[(1 + f_1 + f_2) f_3 - f_1 f_2 \right] . \tag{4.8}$$

In this region $\mathcal{K}_\lambda \sim k_4$ which compensates for the factor $1/k_4$ produced by $\mathcal{F}_{[f]}$. The remaining (finite) integrand is integrated over an area proportional to k_1,

$$\frac{1}{k_1^2} \iint_{③} dk_3 dk_4 \left[\dots \right] \underset{k_4 \to 0}{\sim} \frac{1}{k_1^2} k_1 , \tag{4.9}$$

producing a leading $1/k_1$ behaviour. In region ②, we have $\underline{k}_2, k_4 \lesssim k_1$. The dominant contribution to the functional $\mathcal{F}_{[f]}$ comes from the "doubly divergent" term

$$\frac{1}{\underline{k}_2 k_4}(f_3 - f_1)\,. \tag{4.10}$$

However, the area of integration is now proportional to k_1^2 and we find

$$\frac{1}{k_1^2}\iint_{②} dk_3 dk_4 \frac{1}{\underline{k}_2}\left[\ldots\right] \underset{k_4\to 0}{\sim} \frac{1}{k_1}\,, \tag{4.11}$$

as expected. Additional care must be taken with region ①, due to the apparent "triple divergence" of $\mathcal{F}_{[f]}$. With all momenta soft, the dominant contribution to the integrand is

$$\mathcal{F}_{[f]}\frac{\underline{k}_2}{k} \underset{k_i\to 0}{\sim} -\frac{1}{k_1^2}\frac{(k_1-k_3)(k_1-k_4)}{k_3k_4} = -\frac{1}{k_1^2} + \frac{1}{k_1}\frac{k_3+k_4}{k_3k_4} - \frac{1}{k_3k_4}\,, \tag{4.12}$$

where to simplify the expression in the first step we've used the property $\underline{k}_2 = k_3 + k_4 - k_1$. The first and last terms of the expression in (4.12) can be shown to produce the anticipated $1/k_1$ through similar methods as those described above. Working explicitly through the middle term,

$$\begin{aligned} \frac{1}{k_1^2}\int_0^{k_1} dk_3 \int_{k_1-k_3}^{k_1} dk_4 \frac{k_3+k_4}{k_3k_4} &= \frac{1}{k_1^2}\int_0^{k_1} dk_3 \left[\log\left(\frac{k_1}{k_1-k_3}\right)+1\right] \\ &= \frac{1}{k_1}\,, \end{aligned} \tag{4.13}$$

we find that it does indeed produce the desired $1/k_1$ behaviour.

From this we conclude that a ghost of the IR divergent equilibrium solution is present from the very beginning of the evolution. This informs us that any numerical solution of this Boltzmann equation must take heed of the soft behaviour of its computed distribution function at all times of its evolution. This becomes increasingly apparent when one considers the possible presence of a Bose-Einstein condensate, as discussed in the following section.

4.3 Including the condensate

In order to capture the behaviour (or existence) of Bose-Einstein condensate we must modify the Boltzmann equation as described in Section 3.2. Doing this leads to the following expressions for outgoing and incoming condensate scattering

$$\begin{aligned} C^{\text{out}}_{[f]}(\boldsymbol{k}_1) &= \frac{\lambda^2}{16mE_1}\int_{34}\frac{(2\pi)^4}{E_3E_4}\mathcal{F}^{1c34}_{[f]}\delta^{(4)}(K_1+\underline{K}_2+K_3+K_4) \\ &= \frac{\lambda^2}{64\pi^2}\frac{1}{mE_1k_1}\int_m^E dE_3\,\mathcal{F}^{1c34}_{[f]}\,, \end{aligned} \tag{4.14}$$

$$\begin{aligned} C^{\text{in}}_{[f]}(\boldsymbol{k}_1) &= \frac{\lambda^2}{16mE_1}\int_{24}\frac{(2\pi)^4}{E_2E_4}\mathcal{F}^{12c4}_{[f]}\delta^{(4)}(K_1+K_2+\underline{K}_3+K_4) \\ &= \frac{\lambda^2}{64\pi^2}\frac{1}{mE_1k_1}\int_E^\infty dE_4\,\mathcal{F}^{12c4}_{[f]}\,. \end{aligned} \tag{4.15}$$

To update the number of condensate particles (according to (3.9b)) we take advantage of particle number conservation (see (3.11)) to write

$$\mathcal{R}_{c\,[f]} = -\int_{\boldsymbol{k}}\left(C^{\text{in}}_{[f]} + 2C^{\text{out}}_{[f]}\right)\,, \tag{4.16}$$

allowing us to significantly reduce the computational effort required of each update step.

4.4 Evolution of the system

We now present the results of numerically simulating the evolution of this system of “gluons” under a scalar interaction, following the approach laid out in Chapter 3. Unless otherwise specified, for the results that follow the energy lattice is specified by the parameters $\Lambda_{\text{UV}}/Q = 3$, $m/Q = 0.1$ and $N = 500$.

We begin by looking at the evolution of the regular distribution function. As discussed in Chapter 2, under the Boltzmann equation with Bose statistics an initial condition will evolve to an equilibrium Bose-Einstein distribution with predicted equilibrium parameters $\{\mu, T\}$ (along with a possible condensate). Introducing the transformation

$$g(k) := \log\left(\frac{1+f(k)}{f(k)}\right), \tag{4.17}$$

under which a Bose-Einstein distribution is represented as a straight line, we present an example of such an evolution in Figure 4.3.

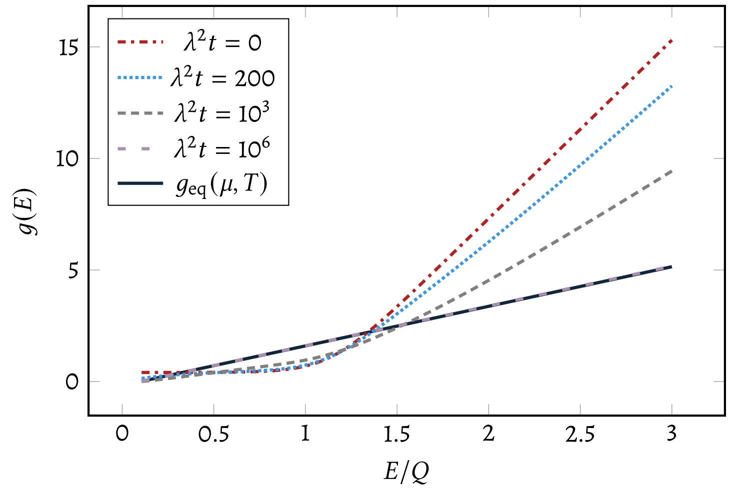

FIGURE 4.3: Distribution function at various times alongside its predicted equilibrium Bose-Einstein distribution ($\{\mu = m, T/Q = 0.56\}$), plotted under the transformation (4.17). The initial condition is fully specified by the parameters $\chi = 2$, $\sigma = 0.125$ and $n_c(0) = 10^{-5}$.

A non-zero initial value of $n_c(0)$ is required for the evolution of the number of condensate particles, as is made clear in Equation 3.9b. In Figure 4.4 we show the evolution of an initial condition with $n_c(0)$ varied from 10^{-3} to 10^{-9}, and see the asymptotic results of the evolution are unaffected.

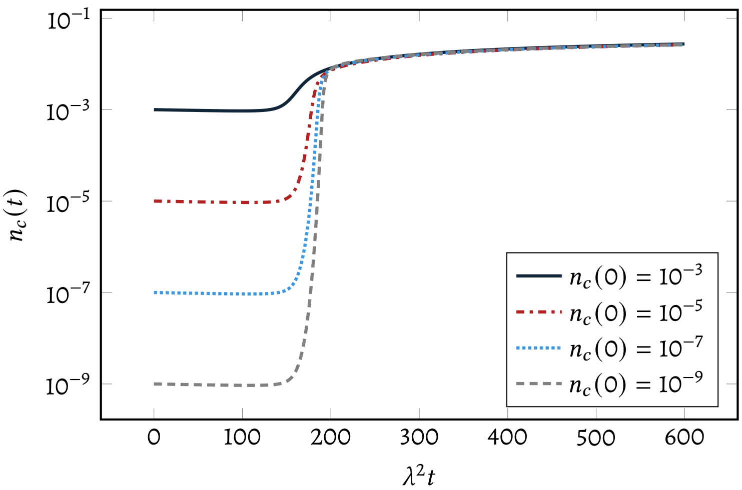

FIGURE 4.4: Evolution of the number of condensate particles, $n_c(t)$, for varied initial value $n_c(0)$. The initial condition is otherwise specified by the parameters $\chi = 5$ and $\sigma = 0.125$.

The behaviour of the evolution is, however, greatly affected by the value of the initial condition parameter χ. This is expected as, given our fixed value of σ, χ controls the population parameter of the initial condition (c.f. Figure 3.4). In Figure 4.5 we show the proportional evolution of the number of condensate particles $n_c(t)/n_{\text{tot}}$, and note the clear difference in behaviour of the underpopulated initial condition given by $\chi = 0.3$ showing the lack of formation of a "macroscopic" condensate.

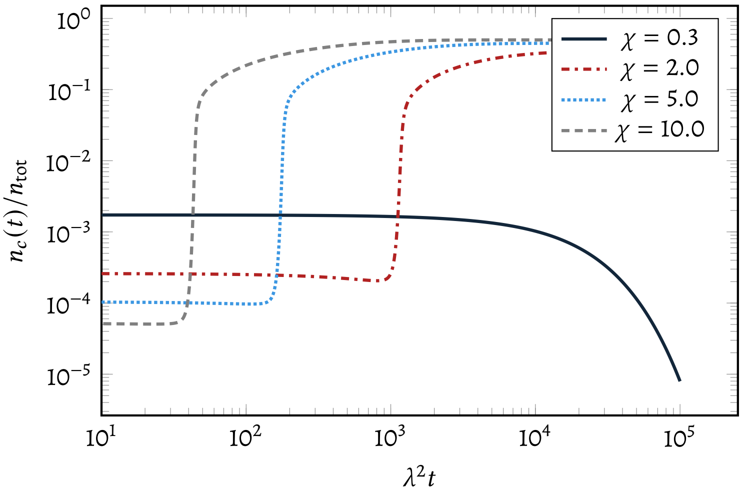

FIGURE 4.5: Evolution of particles in the condensate as a proportion of the total number of particles, $n_c(t)/n_{tot}$ for varied initial particle density as measured by the parameter χ. The initial condition is otherwise specified by the parameters $\sigma = 0.125$ and $n_c(0) = 10^{-5}$.

Chapter 5

QCD Scattering

5.1 The QCD matrix element

For the remainder of this work, we will study a system of gluons interacting through via the strong force. We will consider only elastic gluon-gluon scattering, whose squared-matrix element reads

$$|\mathcal{M}|^2 = 72(4\pi\alpha)^2 \left[3 - \frac{tu}{s^2} - \frac{su}{t^2} - \frac{st}{u^2}\right] \tag{5.1}$$

at Born level [25] (see Fig. 5.1). The dominant scatterings are those involving small momentum transfer between colliding gluons, as can be seen in the terms with denominators t^2 and u^2. This allows one to potentially simplify the form of the matrix element, as we shall see in the following section. Note that due to the crossing symmetry of (5.1), we may identify the t- and u-channel. Thus, when studying the behaviour of the matrix element under soft interactions we will look at $t \ll s$, and infer the behaviour of $u \ll s$ accordingly. For $t \ll s$, we have $u \simeq -s$ and the matrix element is dominated by a term proportional to s^2/t^2. Studying the t dependence of the differential cross section ($d\sigma/dt$), we see a $1/t^2$ divergence

$$\frac{d\sigma}{dt} = \frac{|\mathcal{M}|^2}{16\pi s^2} \underset{t\to 0}{\sim} 72\pi\frac{\alpha^2}{t^2}\,.$$

This, however, results in a divergent transport cross section and will yield nonphysical predictions for physical observables. Therefore we must take into account higher order processes and do so via loop corrections. These corrections enter as a self-energy of the exchange gluon (i.e. the screening of the interaction through the acquisition of a Debye mass μ [26]). We calculate the Debye mass of a system with distribution function $f(\boldsymbol{k})$ as [27]

$$\mu^2 = \alpha \int \frac{d^3k}{(2\pi)^3}\frac{f(\boldsymbol{k})}{k}\,. \tag{5.2}$$

We will look at two methods of screening the IR divergence, a “weak” and a “strong” screening. Both approaches have been used in the literature [17, 28–30]. The weak screening approach is derived from a Hard Thermal Loop (HTL)approximation of the gluon self-energy [31] and

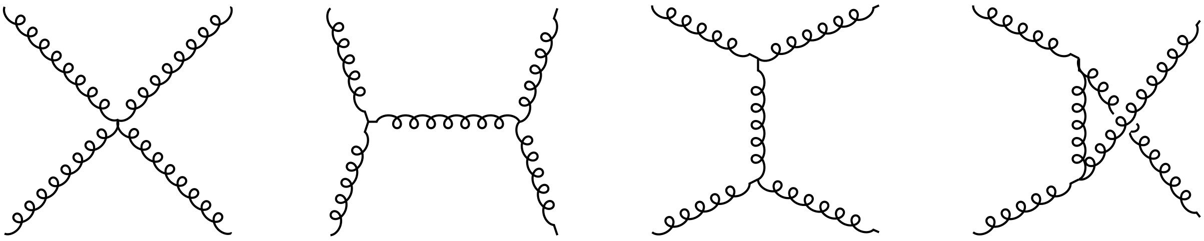

FIGURE 5.1: From left to right: the gluon four vertex, the s-, t- and u-channel diagrams.

modifies

$$\frac{s^2}{t^2} \longrightarrow \frac{s^2}{t(t-\mu^2)}\,. \tag{5.3}$$

This screening mechanism partially preserves the divergence of the matrix element while reducing its strength such as to ensure a finite transport cross section. In contrast, the strong screening approach fully removes the divergence of the matrix element,

$$\frac{s^2}{t^2} \longrightarrow \frac{s^2}{(t-\mu^2)^2}\,. \tag{5.4}$$

This screening is equivalent to the restriction of the range of t through the introduction of an upper cutoff $t^* = -\mu^2$.

5.2 The soft-scattering approximation

As discussed in the previous section, the form of the matrix element (5.1) leads to an overrepresentationof soft scattering events ($t \ll s$). In this regime, one can simplify the Boltzmann equation into a Fokker-Planck equation [5] – thereby trading an integro-differential equation for a more tractable partial differential equation. This is achieved by expressing the outgoing particles' momenta in terms of the momentum transfer $Q = (E_q, \boldsymbol{q})$,

$$\boldsymbol{k}_3 = \boldsymbol{k}_1 + \boldsymbol{q}, \qquad \boldsymbol{k}_4 = \boldsymbol{k}_2 - \boldsymbol{q}\,,$$

and expand the collision term (2.14) in small Q.

Expressing the momenta in terms of $\boldsymbol{q}$ we arrive at an approximation for the distribution function evaluated at these momenta,

$$f_3 = f_1 + q f_1' + O(q^2), \qquad f_4 = f_2 - q f_2' + O(q^2)\,,$$

which leads to

$$\mathcal{F}_{[f]} = q\left(f_1 \bar{f}_1 f_2' - f_2 \bar{f}_2 f_1'\right).$$

Following [29], we're able to rewrite the collision term as a divergence of a current $\mathcal{J}_{[f]}$,

$$\mathcal{D}_t f = \boldsymbol{\nabla} \cdot \mathcal{J}_{[f]} \,, \tag{5.5}$$

which in the case of a homogeneous momentum distribution reads

$$\mathcal{J}_{[f]}(\boldsymbol{k}_1) = \frac{1}{2E_1} \int_2 B(\boldsymbol{k}_1, \boldsymbol{k}_2) \left(f_1 \bar{f}_1 f_2' - f_2 \bar{f}_2 f_1' \right) \tag{5.6}$$

where the directional vector $\hat{\boldsymbol{k}}$ is implied and

$$B(\boldsymbol{k}_1, \boldsymbol{k}_2) = \int \frac{d^3 q}{(2\pi)^3} \frac{q^2}{4E_3 E_4} |\mathcal{M}|^2 \delta(E_1 + E_2 - E_3 - E_4) \,, \tag{5.7}$$

noting $E_3 = E_3(\boldsymbol{k}_1, \boldsymbol{q})$, $E_3 = E_4(\boldsymbol{k}_2, \boldsymbol{q})$.

Considering massless particles and an unscreened matrix element, following [18] we get

$$\mathcal{J}_{[f]}(\boldsymbol{k}_1) = 36\pi\alpha^2 \mathcal{L} \left[I_A f_1' + I_B f_1 \bar{f}_1 \right] , \tag{5.8}$$

Note here the emergence of the Coulomb logarithm $\mathcal{L}$ a divergent integral of the form

$$\mathcal{L} := \int_{k_-}^{k_+} \frac{dk}{k} \,, \tag{5.9}$$

where the cutoffs $k_\pm$ are determined by the equilibrium temperature and screening effects respectively: $k_+ \sim T$, $k_- \sim m_D$. A discussion of the Coloumb logarithm in this context can be found in [32].

Authors [29, 33, 34] have used this approach to study the behaviour of this elastic gluon system, looking particularly at the question of an emergence of a transient Bose-Einsten condensation. This previous work provides valuable points of comparison for the results produced by the differing approach taken in this paper.

5.3 Simplifying the collision term

In the case of a non-trivial matrix element (5.1), the details of the described interactions are encoded in the kernel

$$\mathcal{K}_{\mathcal{M}}(\boldsymbol{k}_1, \boldsymbol{k}_3, \boldsymbol{k}_4) = \int_{s_-}^{s_+} ds \int_{t_-}^{t_+} dt \frac{1}{\sqrt{Q(s, t, \ldots)}} |\mathcal{M}|^2(s, t) \,, \tag{5.10}$$

where, as discussed in Appendix A, Q is a function quadratic in any of its variables s, t, $\boldsymbol{k}_1$, $\boldsymbol{k}_3$ and $\boldsymbol{k}_4$ and the kinematics of the interaction are described in the bounds of the integrals over the Mandelstam invariants s and t.

Focusing on the "weakly screened" t-channel, we note that we can express the matrix element as

$$|\mathcal{M}_t|^2 := \frac{s^2}{t(t-\mu^2)} = \frac{1}{\mu^2}\left(\frac{s^2}{t} - \frac{s^2}{t-\mu^2}\right), \tag{5.11}$$

allowing us to write the kernel

$$\mathcal{K}_t = \frac{1}{\mu^2}\Big(\mathcal{I}(\dots;\mu) - \mathcal{I}(\dots;0)\Big) \tag{5.12}$$

in terms of a master integral

$$\mathcal{I}(\boldsymbol{k}_1, \boldsymbol{k}_3, \boldsymbol{k}_4;\mu) := \int_{s_-}^{s^+} ds \int_{t_-}^{t^+} dt \frac{1}{\sqrt{Q(t,s,\dots)}} \frac{s^2}{t-\mu^2}\,, \tag{5.13}$$

which is calculated in Appendix D.

Chapter 6

Summary and Outlook

In this thesis we have developed numerical scheme capable of solving the relativistic Boltzmann equation for gluons under the assumption of spatial homogeneity and spherically symmetric initial conditions. In particular, we have used the Mandelstam kernel (5.10) to reproduce the known results from the case of scalar interactions (as seen in Chapter 4) and we have generalized this formulation to the case of QCD interactions under an approximation of soft scatterings (as seen in Chapter 5).

In doing so we have numerically tracked the formation of a Bose-Einstein condensate in the case of the scalar interactions. Further numerical work is required to track the expected formation in the QCD case, with the "weakly screened" matrix element (5.11).

Appendix A

Two-body phase space

Considering a function of the participating collision momenta $g(\boldsymbol{k}_1, \boldsymbol{k}_2, \boldsymbol{k}_3, \boldsymbol{k}_4)$, we evaluate the functional

$$\mathcal{G}_{[g]} := \int d\Gamma\, g\,. \tag{A.1}$$

We reduce this sixfold integral following [35]. We re-write the integral over $\boldsymbol{k}_4$ into its manifestly covariant form

$$\int \frac{d^3k_4}{(2\pi)^3}\frac{1}{2E_4} = \int \frac{d^4K_4}{(2\pi)^4}(2\pi)\delta(K_4^2 - m^2)\Theta(E_4)\,, \tag{A.2}$$

and calculate

$$\int_4 \delta^{(4)}(K_1 + K_2 - K_3 - K_4)\, g = 2\pi\delta(\underline{K}_4^2 - m^2)\Theta(\underline{E}_4)\underline{g}\,. \tag{A.3}$$

Note that a dependence on the fixed four-momentum $\underline{K}_4 = K_1 + K_2 - K_3$ is represented by the underline, for example $\underline{E}_4 = E_1 + E_2 - E_3$. We specify the coordinate system by aligning the z-axis with $\boldsymbol{k}_1$ and orienting the zy-plane to contain $\boldsymbol{k}_3$,

$$\begin{aligned}
\boldsymbol{k}_1 &= k_1(0, 0, 1)\,,\\
\boldsymbol{k}_2 &= k_2(\sin\phi\sin\theta_2, \cos\phi\sin\theta_2, \cos\theta_2)\,,\\
\boldsymbol{k}_3 &= k_3(0, \sin\theta_3, \cos\theta_3)\,.
\end{aligned} \tag{A.4}$$

We perform the azimuthal integration over ϕ through the on-shell condition in (A.3). We express the argument of this delta function in terms of the Mandelstam invariants $s = (K_1 + K_2)^2$ and $t = (K_1 - K_3)^2$ as

$$\underline{K}_4^2 - m^2 = s + t - 2m^2 - 2K_2 \cdot K_3\,. \tag{A.5}$$

Evaluating the four-product using (A.4), we find $\underline{K}_4^2 - m^2 = A + B\cos\phi$ where

$$\begin{aligned}
A &= s + t - 2m^2 - 2(E_2E_3 - k_2k_3\cos\theta_2\cos\theta_3)\,,\\
B &= 2k_2k_3\sin\theta_2\sin\theta_3\,.
\end{aligned} \tag{A.6}$$

With this, we evaluate the azimuthal integral

$$\int_0^{2\pi} d\phi\, \delta(A + B\cos\phi) g(\phi) = E_1 \frac{\Theta(Q)}{\sqrt{Q}} \sum_{\pm} g(\phi_\pm) \tag{A.7}$$

where $\phi_\pm = \pi \pm \arccos(A/B)$ and $Q = E_1^2(B^2 - A^2)$. For the remaining angular integrals we change variables from $\{\cos\theta_2, \cos\theta_3\} \longrightarrow \{s, t\}$ defined by

$$\begin{aligned} s &= 2m^2 + 2(E_1E_2 - k_1k_2\cos\theta_2)\,, \\ t &= 2m^2 - 2(E_1E_2 - k_1k_3\cos\theta_3)\,, \end{aligned} \tag{A.8}$$

with Jacobian $4k_1^2k_2k_3$. Thus, defining

$$\mathcal{K}_{[g]} := \int ds \int dt \frac{\Theta(Q)}{\sqrt{Q}} \sum_{\pm} \underline{g}(\phi_\pm)\,, \tag{A.9}$$

and changing variables $E_2 \longrightarrow E_4 = E_1 + E_2 - E_3$, we have

$$\mathcal{G}_{[g]} = \frac{1}{16(2\pi)^4 k_1} \int dE_3\, dE_4\, \mathcal{K}_{[g]}\,. \tag{A.10}$$

The kinematic restrictions of the collision, as represented by $\Theta(Q)$, define the phase space of (A.9). Q, a function quadratic in each of the integration variables, is expressed as $Q(t) = a_t t^2 + b_t t + c_t$, with coefficients

$$\begin{aligned} a_t &= s - (E_3 + E_4)^2\,, \\ b_t &= s^2 - 2s(E_1E_4 + \underline{E}_2E_3 + 2m^2) + 4m^2(E_3 + E_4)^2\,, \\ c_t &= -s(s - 4m^2)(E_1 - E_3)^2\,. \end{aligned} \tag{A.11}$$

As $a < 0$, $Q(t)$ is positive in the interval $[t_-, t_+]$,

$$t_\pm = \frac{-b_t \pm \sqrt{b_t^2 - 4a_tc_t}}{2a_t} =: \frac{-b_t \pm \sqrt{\Delta}}{2a_t}\,. \tag{A.12}$$

Positivity of the discriminant further restricts the phase space, requiring $s \in [s_-, s_+]$ where

$$s_\pm = 2\begin{cases} E_1\underline{E}_2 + m^2 \pm k_1\underline{k}_2 & \text{if } E_1\underline{E}_2 < E_3E_4 \\ E_3E_4 + m^2 \pm k_3k_4 & \text{if } E_1\underline{E}_2 \geq E_3E_4 \end{cases}\,. \tag{A.13}$$

With the kinematic bounds fully specified, the factor $\Theta(Q)$ can be dropped in (A.9) to give

$$\mathcal{K}_{[g]} = \int_{s_-}^{s^+} ds \int_{t_-}^{t^+} dt \frac{1}{\sqrt{Q}} \sum_{\pm} \underline{g}(\phi_\pm) \,. \tag{A.14}$$

Appendix B

Number/energy conserving discretization

To calculate integrals in the form of (3.4) we discretize E_3, E_4 into $N + 1$ linearly spaced points between m and $\Lambda_{\rm UV}$, Then, if E_1 is on this grid we are guaranteed that $\underline{E}_2$ is too, thereby eliminating any need for an interpolation of the integrand. We denote these grid points $\mathbb{E}_i$ ($i \in [0, N]$), where

$$\mathbb{E}_i = m + i\Delta \qquad , \qquad \Delta = \frac{\Lambda_{\rm UV} - m}{N} \,. \tag{B.1}$$

This, additionally, allows us to refer to E_3, E_4 not only by their values but also by their associated indices i, j.

With this we use an equidistant quadrature formula to estimate integrals over energy by

$$\int_m^{\Lambda_{\rm UV}} dE\, g(E) \approx \Delta \sum_{i=0}^{N} W_i\, g(\mathbb{E}_i) \tag{B.2}$$

where the weights W_i depend on the details of the quadrature formula chosen. For the conservation laws to hold exactly for our approximated collision term we must ensure that we preserve the symmetries of the collision term - invariance under the exchange of the two particles in the initial state or the two in the final state and antisymmetry under the exchange of final and initial states. We do this by explicitly reintroducing the energy conserving δ-function,

$$\begin{aligned} \iint_{\mathcal{R}} dE_3 dE_4 \Big\{ \underline{\ldots} \Big\} &= \int dE_3 dE_4 dE_2\, \delta(E_1 + E_2 - E_3 - E_4) \Big\{ \ldots \Big\} \\ &\approx \Delta^2 \sum_{i,j,l=1}^{N} W_i W_j W_l \delta_{k+l-i-j} \Big\{ \ldots \Big\} = \Delta^2 \sum_{i,j=1}^{N} W_i W_j W_{i+j-k} \Big\{ \underline{\ldots} \Big\} , \end{aligned} \tag{B.3}$$

where k is the index corresponding to E_1. Note here we've dropped the zeroth term of the momentum sums. In the calculation of the collision term this point would correspond to the evaluation of the distribution function at the condensate, a potentially singular point. We've taken care of this by explicitly separating the evolution of the regular distribution function from the evolution of the number of particles in the condensate. Thus, we will be evaluating the integrand of $C_{[f]}$ for $E > m$.

From (B.3), for a chosen quadrature scheme, we can read off the weights that should be used in the double sum in order to exactly (or, more precisely, within floating point accuracy) conserve particle and energy density. In this thesis we will use the trapezoidal rule, with weights

$$W_1 = W_N = \frac{1}{2} \qquad , \qquad W_2, W_3, \ldots, W_{N-1} = 1\,. \tag{B.4}$$

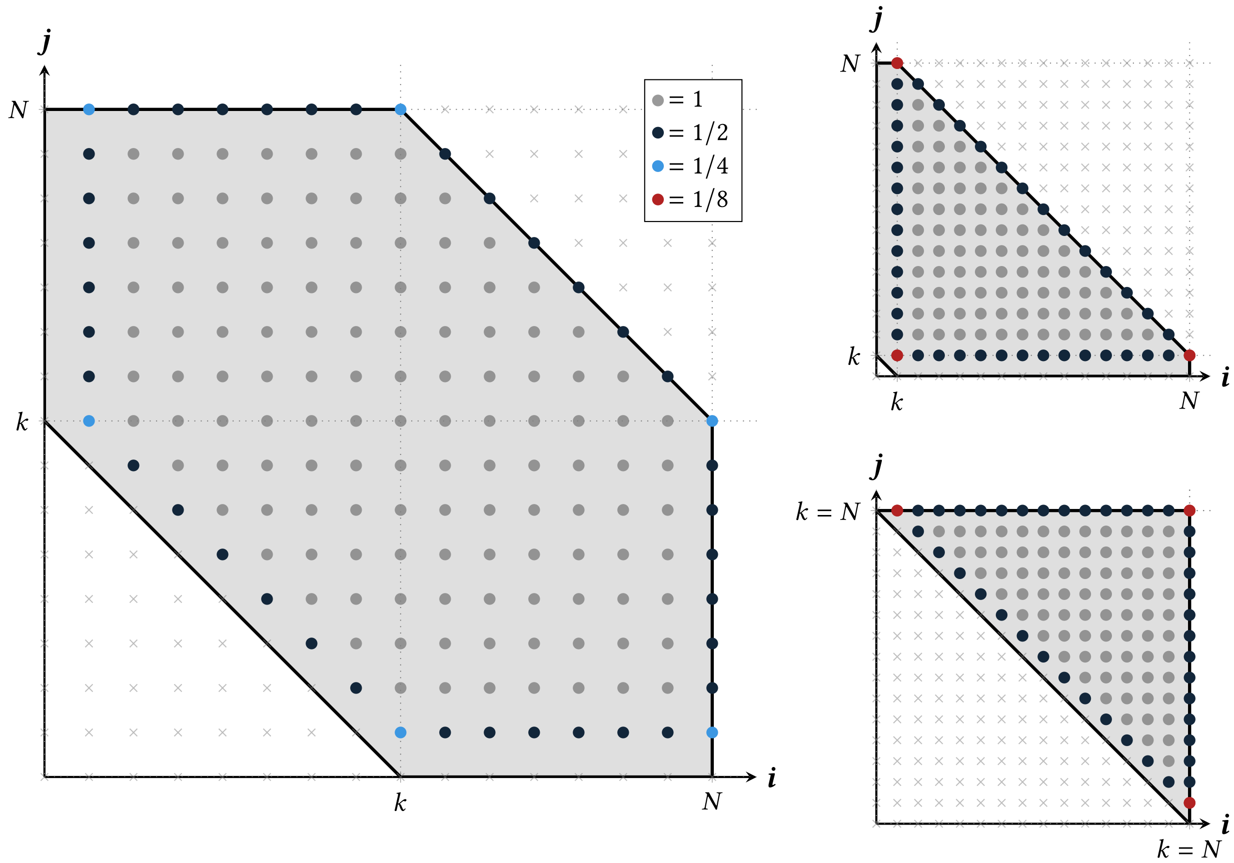

FIGURE B.1: Number/energy conserving trapezoidal quadrature weights evaluated on the energy index phase space i-j, with the edge cases of $k = 1$ (top right) and $k = N$ (bottom right) pictured on the right.

Appendix C

Critical population on an equidistant grid

On a finite grid the *lattice* values of the particle and energy density must be conserved

$$\varepsilon_{\rm eq}(T,\nu) = \frac{\Delta^3}{2\pi^2}\sum_{i=1}^{N} i^2 f_{{\rm B}i} \stackrel{!}{=} \underline{\varepsilon_{\rm in}}\,, \tag{C.1a}$$

$$n_{\rm eq}(T,\nu) = \frac{\Delta^4}{2\pi^2}\sum_{i=1}^{N} i^3 f_{{\rm B}i} \stackrel{!}{=} \underline{n_{\rm in}}\,, \tag{C.1b}$$

where we've taken, without loss of generality, $m = 0$ such that $\mathbb{E}_i = i\Delta$ and defined $f_{{\rm B}i} := f_{\rm B}(\mathbb{E}_i/T+\nu)$.

As in Section 2.3, these conditions define two lines in the ν-T plane with gradients

$$\partial_T\left[\varepsilon_{\rm eq}(T,\nu)\right] = \partial_T\varepsilon_{\rm eq}(T,\nu) + \partial_\nu\varepsilon_{\rm eq}(T,\nu)\partial_T\nu = 0$$

$$\implies \partial_T\nu_\varepsilon = \frac{\Delta}{T^2}\frac{\sum_i i^4 f'_{{\rm B}i}}{\sum_j j^3 f'_{{\rm B}j}}\,, \tag{C.2a}$$

and

$$\partial_T\left[n_{\rm eq}(T,\nu)\right] = \partial_T n_{\rm eq}(T,\nu) + \partial_\nu n_{\rm eq}(T,\nu)\partial_T\nu = 0$$

$$\implies \partial_T\nu_n = \frac{\Delta}{T^2}\frac{\sum_i i^3 f'_{{\rm B}i}}{\sum_j j^2 f'_{{\rm B}j}}\,, \tag{C.2b}$$

where $f'_{\rm B}(x) = f_{\rm B}(x)\underline{f_{\rm B}}(x)$. To show that the critical is unique, we show that $\partial_T\nu_\varepsilon > \partial_T\nu_n$ always; implying that the intersection of the two lines at $\nu = 0$ is unique. We recognise this as the following problem

$$\sum_{j,k=1}^{N} j^4k^2 c_j c_k \stackrel{?}{>} \sum_{j,k=1}^{N} j^3k^3 c_j c_k\,,$$

or, equivalently

$$Z := \sum_{j,k=1}^{N} c_j c_k j^3 k^2 (j-k) \stackrel{?}{>} 0\,. \tag{C.3}$$

We begin by noting that the coefficients c_j, c_k are strictly positive since the Bose distribution function is strictly positive. Then we note that all terms with $j = k$ are zero. Thus, we can split the sum into one over terms with $j > k$ and terms with $j < k$ as

$$Z = \sum_{j>k}^{N} c_j c_k j^3 k^2 (j-k) + \sum_{j>k}^{N} c_j c_k j^3 k^2 (j-k)\,.$$

Relabeling $j \leftrightarrow k$ in the second sum and grouping terms we find

$$\begin{aligned} Z &= \sum_{j>k}^{N} c_j c_k j^2 k^2 \Big[j(j-k) - k(j-k) \Big]\,. \\ &= \sum_{j>k}^{N} c_j c_k j^2 k^2 \Big[(j-k)^2 \Big] > 0\,. \quad \square \end{aligned} \tag{C.4}$$

Appendix D

Master integral: gluon-gluon collisions

As discussed in Chapter 5 it is possible to relate relevant collision kernels to the master integral

$$\mathcal{I}(\boldsymbol{k}_1, \boldsymbol{k}_3, \boldsymbol{k}_4; \mu) := \int_{s_-}^{s^+} ds \int_{t_-}^{t^+} dt \frac{1}{\sqrt{Q(t, s, \dots)}} \frac{s^2}{t - \mu^2}, \tag{D.1}$$

where Q (a function quadratic in any of its variables) and the integration bounds of the integrals over the Mandelstam invariants s and t are discussed in Appendix A. Note that in the calculations that follow, for notational convenience we shall suppress the additional arguments of the integrand functions, i.e. $Q(t, s, \dots) \to Q(t, s)$.

We begin by performing the definite integral over t, recalling $Q(t_+, s) = Q(t_-, s) = 0$, to find

$$\int_{t_-}^{t^+} dt \frac{1}{\sqrt{Q(t, s)}} \frac{s^2}{t - \mu^2} = -\pi \frac{s^2}{\sqrt{\widetilde{Q}(s)}}, \tag{D.2}$$

where $\widetilde{Q}(s) = -Q(t = \mu^2, s) = a_s s^2 + b_s s + c_s$ with coefficients

$$\begin{aligned} a_s &= (E_1 - E_3)^2 - \mu^2, \\ b_s &= -4m^2(E_1 - E_3)^2 - \mu^4 + 2\mu^2(E_1 E_4 + \underline{E}_2 E_3 + 2m^2), \\ c_s &= \mu^2(\mu^2 - 4m^2)(E_3 + E_4)^2. \end{aligned} \tag{D.3}$$

We then compute the integral over s to get the final result

$$\mathcal{I}(\boldsymbol{k}_1, \boldsymbol{k}_3, \boldsymbol{k}_4; \mu) = \frac{\pi}{4a_s^2} \left[(3b_s - 2a_s s)\sqrt{\widetilde{Q}(s)} + \frac{4a_s c_s - 3b_s^2}{2\sqrt{-a_s}} \arcsin\left(\frac{b_s + 2a_s s}{b_s^2 - 4a_s c_s} \right) \right]_{s_-}^{s^+}, \tag{D.4}$$

where $s_\pm$ are defined in Eq. (A.13).

Bibliography

[1] J. Adams et al. "Experimental and theoretical challenges in the search for the quark–gluon plasma: The STAR Collaboration's critical assessment of the evidence from RHIC collisions". In: *Nuclear Physics A* 757.1–2 (2005), 102–183. ISSN: 0375-9474. DOI: 10.1016/j.nuclphysa.2005.03.085. URL: http://dx.doi.org/10.1016/j.nuclphysa.2005.03.085.

[2] K. Aamodt et al. "Elliptic Flow of Charged Particles in Pb-Pb Collisions atsNN=2.76TeV". In: *Physical Review Letters* 105.25 (2010). ISSN: 1079-7114. DOI: 10.1103/physrevlett.105.252302. URL: http://dx.doi.org/10.1103/PhysRevLett.105.252302.

[3] B Jacak and P Steinberg. "Creating The Perfect Liquid In Heavy-Ion Collisions". In: *Physics Today* 63.5 (May 2010). ISSN: 0031-9228. DOI: 10.1063/1.3431330. URL: https://www.osti.gov/biblio/988764.

[4] F. Schwabl and W.D. Brewer. *Statistical Mechanics*. Advanced Texts in Physics. Springer Berlin Heidelberg, 2006. ISBN: 9783540323433. URL: https://books.google.co.za/books?id=7VnKAW284PgC.

[5] E.M. Lifshits et al. *Physical Kinetics*. Course of theoretical physics. Pergamon Press, 1981. ISBN: 9780080264806. URL: https://books.google.co.za/books?id=tQNTIOPaJukC.

[6] M. Kardar. *Statistical Physics of Particles*. Cambridge University Press, 2007. ISBN: 9781139464871. URL: https://books.google.co.za/books?id=1WlFhiz5UjwC.

[7] E. A. Uehling and G. E. Uhlenbeck. "Transport Phenomena in Einstein-Bose and Fermi-Dirac Gases. I". In: *Phys. Rev.* 43 (7 1933), pp. 552–561. DOI: 10.1103/PhysRev.43.552. URL: https://link.aps.org/doi/10.1103/PhysRev.43.552.

[8] E. A. Uehling. "Transport Phenomena in Einstein-Bose and Fermi-Dirac Gases. II". In: *Phys. Rev.* 46 (10 1934), pp. 917–929. DOI: 10.1103/PhysRev.46.917. URL: https://link.aps.org/doi/10.1103/PhysRev.46.917.

[9] Lester Lees. "Kinetic Theory Description of Rarefied Gas Flow". In: *Journal of the Society for Industrial and Applied Mathematics* 13.1 (1965), pp. 278–311. ISSN: 03684245. URL: http://www.jstor.org/stable/2946405.

[10] M. H. Anderson et al. “Observation of Bose-Einstein Condensation in a Dilute Atomic Vapor”. In: *Science* 269.5221 (1995), pp. 198–201. ISSN: 0036-8075. DOI: 10.1126/science.269.5221.198. eprint: https://science.sciencemag.org/content/269/5221/198.full.pdf. URL: https://science.sciencemag.org/content/269/5221/198.

[11] Jordan M. Gerton et al. “Direct observation of growth and collapse of a Bose–Einstein condensate with attractive interactions”. In: *Nature* 408.6813 (2000), 692–695. ISSN: 1476-4687. DOI: 10.1038/35047030. URL: http://dx.doi.org/10.1038/35047030.

[12] W Ketterle et al. “Bose–Einstein condensation of ultracold atomic gases”. In: *Physica Scripta* T66 (1996), pp. 31–37. DOI: 10.1088/0031-8949/1996/t66/004. URL: https://doi.org/10.1088.

[13] Jan Klaers et al. “Bose–Einstein condensation of photons in an optical microcavity”. In: *Nature* 468.7323 (2010), 545–548. ISSN: 1476-4687. DOI: 10.1038/nature09567. URL: http://dx.doi.org/10.1038/nature09567.

[14] David Aveline et al. “Observation of Bose–Einstein condensates in an Earth-orbiting research lab”. In: *Nature* 582 (2020), pp. 193–197. DOI: 10.1038/s41586-020-2346-1.

[15] Francois Gelis et al. “The Color Glass Condensate”. In: *Annual Review of Nuclear and Particle Science* 60.1 (2010), 463–489. ISSN: 1545-4134. DOI: 10.1146/annurev.nucl.010909.083629. URL: http://dx.doi.org/10.1146/annurev.nucl.010909.083629.

[16] F. Scardina et al. “Relativistic Boltzmann transport approach with Bose-Einstein statistics and the onset of gluon condensation”. In: *Physical Review C* 90.5 (2014). ISSN: 1089-490X. DOI: 10.1103/physrevc.90.054904. URL: http://dx.doi.org/10.1103/PhysRevC.90.054904.

[17] Zhe Xu et al. “Thermalization of Gluons with Bose-Einstein Condensation”. In: *Physical Review Letters* 114.18 (2015). ISSN: 1079-7114. DOI: 10.1103/physrevlett.114.182301. URL: http://dx.doi.org/10.1103/PhysRevLett.114.182301.

[18] Jean-Paul Blaizot et al. “Bose–Einstein Condensation and Thermalization of the Quark Gluon Plasma”. In: *Nucl. Phys. A* 873 (2012), pp. 68–80. DOI: 10.1016/j.nuclphysa.2011.10.005. arXiv: 1107.5296 [hep-ph].

[19] J.I. Kapusta. *Finite-Temperature Field Theory*. Cambridge Monographs on Mathematical Physics. Cambridge University Press, 1993. ISBN: 9780521449458. URL: https://books.google.co.za/books?id=nT2kbcDtMl8C.

[20] Thomas Epelbaum et al. “Properties of the Boltzmann equation in the classical approximation”. In: *Physical Review D* 90.12 (2014). ISSN: 1550-2368. DOI: 10.1103/physrevd.90.125032. URL: http://dx.doi.org/10.1103/PhysRevD.90.125032.

[21] J. Berges et al. "Basin of attraction for turbulent thermalization and the range of validity of classical-statistical simulations". In: *Journal of High Energy Physics* 2014.5 (2014). ISSN: 1029-8479. DOI: 10.1007/jhep05(2014)054. URL: http://dx.doi.org/10.1007/JHEP05(2014)054.

[22] Robert Lacaze et al. "Dynamical formation of a Bose–Einstein condensate". In: *Physica D: Nonlinear Phenomena* 152 (2001), pp. 779–786. DOI: 10.1016/S0167-2789(01)00211-1.

[23] E. Fehlberg. *Low-order Classical Runge-Kutta Formulas with Stepsize Control and Their Application to Some Heat Transfer Problems*. NASA technical report. National Aeronautics and Space Administration, 1969. URL: https://books.google.co.za/books?id=IMaJw5g4hGkC.

[24] D. V. Semikoz and I. I. Tkachev. "Condensation of bosons in the kinetic regime". In: *Physical Review D* 55.2 (1997), 489–502. ISSN: 1089-4918. DOI: 10.1103/physrevd.55.489. URL: http://dx.doi.org/10.1103/PhysRevD.55.489.

[25] Roger Cutler and Dennis Sivers. "Quantum-chromodynamic gluon contributions to large-p_T reactions". In: *Phys. Rev. D* 17 (1 1978), pp. 196–211. DOI: 10.1103/PhysRevD.17.196. URL: https://link.aps.org/doi/10.1103/PhysRevD.17.196.

[26] Joseph I. Kapusta and Charles Gale. *Finite-Temperature Field Theory: Principles and Applications*. 2nd ed. Cambridge Monographs on Mathematical Physics. Cambridge University Press, 2006. DOI: 10.1017/CBO9780511535130.

[27] Aleksi Kurkela and Guy D. Moore. "Thermalization in weakly coupled nonabelian plasmas". In: *Journal of High Energy Physics* 2011.12 (2011). ISSN: 1029-8479. DOI: 10.1007/jhep12(2011)044. URL: http://dx.doi.org/10.1007/JHEP12(2011)044.

[28] S. M. H. Wong. "Thermal and chemical equilibration in relativistic heavy ion collisions". In: *Physical Review C* 54.5 (1996), 2588–2599. ISSN: 1089-490X. DOI: 10.1103/physrevc.54.2588. URL: http://dx.doi.org/10.1103/PhysRevC.54.2588.

[29] Jean-Paul Blaizot and Jinfeng Liao. "Gluon transport equations with condensate in the small angle approximation". In: *Nuclear Physics A* 949 (2016), 35–47. ISSN: 0375-9474. DOI: 10.1016/j.nuclphysa.2015.08.004. URL: http://dx.doi.org/10.1016/j.nuclphysa.2015.08.004.

[30] André Peshier. "Turning on the charm". In: *Nuclear Physics A* 888 (2012), 7–22. ISSN: 0375-9474. DOI: 10.1016/j.nuclphysa.2012.05.012. URL: http://dx.doi.org/10.1016/j.nuclphysa.2012.05.012.

[31] Eric Braaten and Robert D. Pisarski. "Soft amplitudes in hot gauge theories: A general analysis". In: *Nuclear Physics B* 337.3 (1990), pp. 569 –634. ISSN: 0550-3213. DOI: https://doi.org/10.1016/0550-3213(90)90508-B. URL: http://www.sciencedirect.com/science/article/pii/055032139090508B.

[32] Jefferson Bjoraker and Raju Venugopalan. “From a colored glass condensate to the gluon plasma: Equilibration in high energy heavy ion collisions”. In: *Physical Review C* 63.2 (2001). ISSN: 1089-490X. DOI: 10.1103/physrevc.63.024609. URL: http://dx.doi.org/10.1103/PhysRevC.63.024609.

[33] Jean-Paul Blaizot, Jinfeng Liao, and Larry McLerran. “Gluon transport equation in the small angle approximation and the onset of Bose–Einstein condensation”. In: *Nuclear Physics A* 920 (2013), 58–77. ISSN: 0375-9474. DOI: 10.1016/j.nuclphysa.2013.10.010. URL: http://dx.doi.org/10.1016/j.nuclphysa.2013.10.010.

[34] Brent Harrison and Andre Peshier. “Bose-Einstein Condensation from the QCD Boltzmann Equation”. In: *Particles* 2.2 (2019), pp. 231–241. DOI: 10.3390/particles2020016.

[35] Stéphane Peigné and André Peshier. “Collisional energy loss of a fast muon in a hot QED plasma”. In: *Physical Review D* 77.1 (2008). ISSN: 1550-2368. DOI: 10.1103/physrevd.77.014015. URL: http://dx.doi.org/10.1103/PhysRevD.77.014015.